Protein J (2007) 26:491–498
DOI 10.1007/s10930-007-9090-3

Thermal-unfolding Reaction of Triosephosphate Isomerase from *Trypanosoma cruzi*

Edgar Mixcoha-Hernández · Liliana M. Moreno-Vargas · Arturo Rojo-Domínguez · Claudia G. Benítez-Cardoza

Published online: 1 September 2007

Abstract Thermal denaturation of triosephosphate isomerase from *Trypanosoma cruzi* was studied by circular dicrhoism and fluorescence spectroscopies. The unfolding transition was found to be highly irreversible even at the very early stages of the reaction. Kinetic studies, allowed us to identify consecutive reactions. Firstly, only the tryptophan environment is altered. Next, changes on the secondary structure and hydrophobic surface exposure measured by 1-anilino-8-naphthalenesulfonate (ANS) binding were observed. Further conformational changes imply additional modifications on the secondary and tertiary structures and release of the hydrophobic dye leading to the formation of the unfolded state that is prone to aggregate.

Keywords Triosephosphate isomerase · Thermal unfolding kinetics · Molten globule · Circular dichroism · Irreversibility

Edgar Mixcoha-Hernández and Liliana M. Moreno-Vargas contributed equally to this work

E. Mixcoha-Hernández · C. G. Benítez-Cardoza (✉)
Laboratorio de Investigación Bioquímica, Programa Institucional en Biomedicina Molecular ENMyH-IPN, Guillermo Massieu Helguera No. 239, La Escalera Ticoman 07320 D.F, Mexico
e-mail: beni1972uk@yahoo.com.mx

L. M. Moreno-Vargas · A. Rojo-Domínguez
Área de Biofisicoquímica, Departamento de Química, Universidad Autónoma Metropolitana-Iztapalapa, Apartado Postal 55–534, Iztapalapa 09340 D.F, Mexico

A. Rojo-Domínguez
Departamento de Ciencias Naturales, Universidad Autónoma Metropolitana-Cuajimalpa, Pedro Antonio de los Santos 84, San Miguel Chapultepec 11850 D.F, Mexico

Abbreviations

TIM	Triosephosphate isomerase
TcTIM	Triosephosphate isomerase from *Trypanosoma cruzi*
TbTIM	Triosephosphate isomerase from *Trypanosoma brucei*
yTIM	Yeast triosephosphate isomerase
CD	Circular dichroism
Tris	Tris(hydroxy-methyl) aminomethane
Gdn-HCl	Guanidine hydrochloride
TEA	Triethanolamine
SCM	Spectral centre of mass

1 Introduction

About 10% of all the enzymes of known structure share the TIM-barrel scaffold [1]. The barrel consists of eight parallel β-strands connected by eight loops to the same number of α-helices. The β-strands form the internal part of the barrel, surrounded by the helices [2]. Amongst TIM-barrel proteins we can find several functions such as: oxido-reductases, transferases, isomerases and hydrolases, among others. A characteristic of these proteins is that despite of showing a common fold, they diverge in their sequences. However, the active site is regularly at the same region of the enzymes, formed by the loops. The relative abundance within the database has led to a proposal that this scaffold is possibly favoured in terms of folding properties or stability [3].

The folding/unfolding mechanism of several TIM barrels has been studied in detail [4–6]. For example, the urea-induced equilibrium unfolding of the alpha-subunit of tryptophan synthase (αTS) from *Escherichia coli* can be

described by a four-state model, $N \leftrightarrow I_1 \leftrightarrow I_2 \leftrightarrow U$, involving two highly populated intermediates, I_1 and I_2 [4, 7]. It has been reported that I_2, is similar to N and I_1, and they share a globular structure while U has a more random coil-like form [4]. More recently, Rojsajjakul and co-workers [8] have demonstrated the existence of two intermediates, one of them, populated at 3 M urea, that keeps considerable secondary structure. The other intermediate showed a structure moiety formed by its first four beta strands and three helices and is populated at higher urea concentrations (4–7 M).

Another TIM barrel protein where folding/unfolding reaction has been studied is imidazol-glycerol phosphate synthase subunit HisF, that is involved in histidine biosynthesis. It has been proposed that this enzyme might have an stable nucleus, resistant to proteolysis, in the C-terminal region $(\alpha/\beta)_{5-8}$ [9].

The unfolding pathway induced by guanidinium hydrochloride (Gdn-HCl) of TIMs from *Bacillus stearothermophilus* [10], *Thermotoga maritime* [11], rabbit [12–14], *Plasmodium falciparum* [15], *Saccharomyces cerevisiae* [16–18], *Leishmania mexicana* [19], *Trypanosoma brucei* [20] and *Trypanosoma cruzi* [6] have been studied in detail. It has been found that, although the crystallographic three-dimensional structures of these enzymes are highly similar, the equilibrium unfolding pathways of homologous TIMs by Gdn-HCl are different. Furthermore, it is noticeable that two trypanosomatid TIMs show different behaviour with respect to inactivation with the same sulfhydryl reagents even though they share a percentage of identity in their sequences of 74% [20, 21]. The equilibrium unfolding of TbTIM [20], was found to be complex and irreversible. In contrast, studies on TcTIM, showed a reversible unfolding reaction that involved two unfolding stable intermediates; an expanded, non-native dimer and a partially expanded monomer. Also the reversible denaturation and renaturation of TIM from baker's yeast (*S. cerevisiae*) induced by Gdn-HCl and urea have been characterized. The simplest equilibrium pathway was found to be a three-state process involving an inactive and expanded monomer [18].

Furthermore, the thermal denaturation of several TIMs has also been studied. In 2001 it was presented a comprehensive analysis of the folding mechanism of triosephospahte isomerase from baker's yeast (yTIM) by spectroscopic and calorimetric methods [22]. It was found that yTIM showed a reversible thermal transition carried out at low protein concentration. However, under those conditions, the denaturation–renaturation cycle exhibited marked hysteresis. In addition it was found that the use of lower scanning rates originated marked irreversibility. Kinetic studies indicated that denaturation of the enzyme likely consists of an initial first-order reaction that forms thermally unfolded (U) TIM, followed by irreversibility-inducing reactions which are probably linked to aggregation of the unfolded protein. As judged from CD measurements, U keeps residual secondary structure but lacks most of the tertiary interactions present in native yTIM. It was concluded that an extensive exposure of surface area occurs when U is formed. It was found that U returns into native like TIM through a second-order reaction in which the association of the subunits is coupled to the recovery of the secondary structure. More recently, it has been established that conserved cysteine 126 in triosephosphate isomerase is required not for enzymatic activity but for proper folding and stability [23].

Up to now, several evidences have been found that show that proteins sharing the TIM barrel topology do not present a common folding mechanism. Different folding pathways have been reported when using different denaturation agents, even for a protein from the same biological source. Therefore, more studies in this field are required in order to understand the reason why the folding/unfolding reaction of TIM barrel proteins might not be conserved. In this paper, we have studied the thermal unfolding mechanism of triosephosphate isomerase from *T. cruzi*. We compare the results with the mechanisms proposed for the thermal denaturation of other TIMs. To our knowledge, this is the first report showing the temperature-induced mechanism of TcTIM.

2 Materials and Methods

2.1 Materials

TcTIM was produced and purified as described by Ostoa-Saloma and coworkers [24]. Concentrations of protein solutions were determined from their absorbencies at 280 nm, using the absorption coefficient reported for TcTIM (ε = 34,950 M^{-1} cm^{-1}) [25]. TIM solutions were prepared at a concentration of 0.010 mg mL^{-1}. Unless otherwise stated, studies were carried out in a buffer solution of 50 mM phosphate adjusted to pH 7.4 (at 25 °C) with NaOH. All reactants were of analytical grade. The water used was distilled and deionized. In all cases, curves are reported as the average of at least two independent experiments. All the assays were carried out using the same lot of protein. Additionally, in order to verify the data, all the experiments were repeated using a different protein lot.

2.2 Thermal Transitions Monitored by Circular Dichroism Spectroscopy

CD measurements were performed as described in a previous paper [22]. Briefly, measurements were performed using a JASCO J-715 spectropolarimeter (Jasco Inc.,

Easton, MD) equipped with a PTC-348WI Peltier-type cell holder for temperature control and magnetic stirring. Thermal denaturation transitions were tracked by examining the ellipticity changes at a wavelength of 220 nm, while the sample temperature was increased at constant rate. Heating rates varied from 0.5 to 4.0 °C min^{-1}, and 1.0 cm path-length cells were used. Ellipticities are reported as mean residue ellipticity [θ].

2.3 Denaturation Kinetics

The kinetics of secondary-structure changes upon TIM thermal denaturation were followed by changes in ellipticity at 220 nm. Cells of 1.0 cm path-length were filled up to 98% of their total volume (3.0 mL) with the phosphate buffer. After temperature equilibration, the necessary amount of concentrated TcTIM solution was added to complete the cell volume. Samples were vigorously stirred to promote rapid mixing and temperature equilibration. Under these conditions the dead time of experiments was less than 10 s. Unfolding data were fitted to a biphasic exponential decay equation, $\theta_t = \theta_f + A_1 \exp(-k_{u1}t) + A_2 \exp(-k_{u2}t)$ where θ_t is the ellipticity measured at time t, θ_f is the final ellipticity value, A_1 and A_2 represent the amplitudes of each phase, and k_{u1} and k_{u2} are the unfolding rate constants for each phase.

2.4 Fluorescence

Fluorescence experiments were carried out in a PC1 spectrofluorometer from ISS (Champaign, IL). This instrument is equipped with a Peltier-type cell holder for temperature control. All the experiments were obtained using cells of 1.0 cm path-length. Samples were excited at 280 nm (otherwise stated). Emission spectra were collected from 300 to 400 nm. The fluorescence spectral centre of mass (SCM) was calculated from intensity data (I_λ) obtained at different wavelengths (λ) using: $SCM = \Sigma (\lambda * I_\lambda)/\Sigma I_\lambda$. The kinetic experiments were performed similarly to the circular dichroism assays; in this case excitation and emission wavelengths were 280 and 320 nm respectively. Unfolding data were fitted to double or triple exponential decay equations.

2.5 1-Anilino-8-naphthalenesulfonate (ANS) Fluorescence

The binding of the hydrophobic dye ANS was measured by fluorescence spectroscopy. The excitation wavelength was 380 nm and emission was collected at 497 nm. ANS was used under saturating concentrations (40 μM). The procedure to start the kinetic experiments was similar to the described for circular dichroism and intrinsic fluorescence.

3 Results and Discussion

3.1 Thermal Transitions of TcTIM Denaturation

Firstly, the thermal denaturation of TcTIM was performed using TRIS buffer 50 mM at pH 7.4 (pH adjusted at 25 °C, data not shown). In this case, the CD signal showed a very large slope in the pre-denaturation region of the curve (before the denaturation process started). It is important to mention that the pKa of TRIS strongly depends on temperature, and significant changes on pH could have occurred while heating the protein solution. Also, this observation might reflect instability of the secondary structure of the protein in the presence of TRIS buffer, or aggregation of the sample. Additionally, unpublished results of our group have shown similar behaviour with some other buffers such as TEA. When the same scanning was carried out in phosphate buffer, keeping the rest of the experimental conditions, it was observed that the slope diminished greatly. This finding confirms that the presence of phosphate ion can be helpful for the stability of the protein. Therefore, it was decided to perform all the experiments in phosphate buffer. The temperature at the middle of the denaturation transition showed only a slight variation within the phosphate and TRIS buffers, at the same pH.

Thermal denaturation of TcTIM was followed by monitoring the ellipticity at 220 nm at constant heating-rates. After the thermal denaturation transitions went to completion, the protein solutions were cooled down up to 30 °C either at the same scan speed; or by quickly reducing the temperature of the sample. Figure 1 shows the transition curves obtained with TcTIM solutions at 0.010 mg mL^{-1} in phosphate buffer (50 mM), pH 7.4, at heating rates of 0.5, and 4 °C min^{-1} and the curve observed when cooling down the sample at a scan speed of 4 °C min^{-1}. It can be seen that secondary structure is not recovered upon cooling. The reversibility of the secondary structure was not achieved in none of the cases. To further explore if the unfolding reaction was reversible or not, the sample was heated for 1 min at 64 °C. Under these conditions, the secondary structure of the native protein disappeared as revealed by the CD signal; immediately after the sample was cooled down, to 30 °C and the secondary structure of the native polypeptide was not recovered. This indicates that the thermal denaturation of TcTIM is highly irreversible even at the very early stages of the reaction.

From Fig. 1, it is also clear that the transition at 0.5 °C min^{-1} appears at lower temperatures than that of 4 °C min^{-1}. This resembles a common result in transitions under kinetic control [26–28]. In addition, the lower heating-rate leads to larger changes in the far-UV CD transition, probably indicating aggregation of the sample. In all cases, aggregation of the protein solutions was confirmed spectrofotometrycally by light scattering at wavelengths higher than 300 nm (data not shown). These findings strongly suggest that irreversibility of the thermal denaturation reaction of TcTIM under the experimental conditions tested could be due to aggregation of the unfolded conformation.

The thermal transition was also studied at higher protein concentrations, such as 0.020 mg mL^{-1} (data not shown). In that case, larger changes in the far-UV CD spectra and transition curves, were observed, *i.e.* the CD signal approached to cero upon thermal treatment of the samples. This finding indicates that higher concentrations of protein might promote sample aggregation.

Values of the apparent enthalpy (ΔHap) were obtained as described by Tello-Solís and Hernandez-Arana [28]. The ΔHap, from four independent experiments, were rather insensitive to variation of heating rate. The average ΔHap, from experiments at 0.5, 1, 2, and 4 °Cmin^{-1} was 420 ± 30 kJ mol^{-1}, which corresponds to 0.84 kJ mol^{-1} of amino acid residue. Even though the thermal unfolding reaction of TcTIM is highly irreversible the ΔHap could still be a trustful thermodynamic parameter, if the exothermic effects from aggregation were not very large [29, 30]. In comparison, this value is about a half to the denaturation enthalpy observed for yTIM 1.5 ± 0.4 kJ mol^{-1} of amino acid residue [22]. According to this thermodynamic criterion TcTIM unfolding process seems to be less cooperative and suggests that it might include intermediate species or involve residual structure on the unfolded species.

3.2 Denaturation Kinetics

The time course of TcTIM denaturation at constant temperature was examined by changes in far UV-CD at 220 nm, at different temperatures. Figure 2 shows three of the kinetic curves obtained (56.0, 58.1 and 63.7 °C). In all cases, double exponential decay curves fitted well to experimental data. This might indicate the presence of at least one kinetic intermediate. The values of ellipticity were extrapolated to time zero and showed to be very similar to those expected for the native protein. These results indicate that if there is a fast kinetic phase (lost during the dead time of the experiment), it does not involve significant secondary-structure changes. From the fitting of the data the rate constants associated to the unfolding reaction were obtained.

3.3 Fluorescence

Further characterization of the time-course of TcTIM thermal-denaturation was achieved by fluorescence experiments. Kinetic curves constructed from the intensities of the emission measured at 320 nm wavelength, at some of the temperatures studied, are shown in Fig. 3. Kinetic curves, followed by fluorescence emission, show

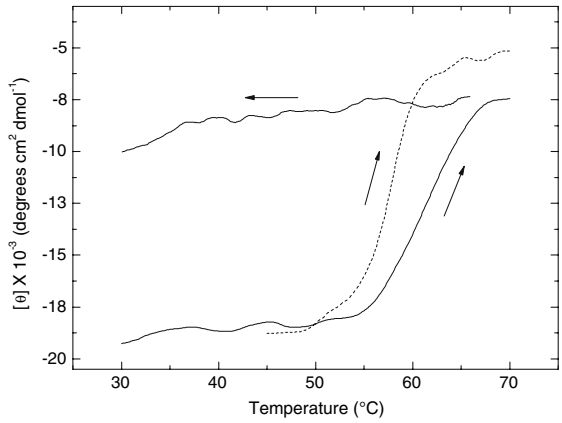

Fig. 1 Heating and cooling profiles of TcTIM in phosphate buffer at pH 7.4. Transitions were obtained by recording the ellipticity of the sample at 220 nm. Heating or cooling rates were 0.5 °C min^{-1} (dashed line) and 4 °C min^{-1} (continuous line). Protein concentration was 0.010 mg mL^{-1}

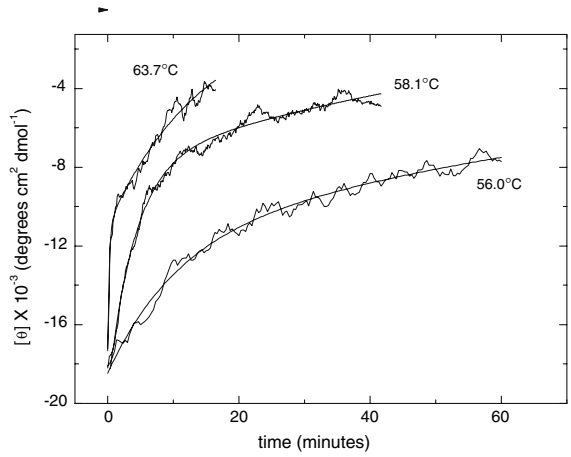

Fig. 2 Kinetics of thermal denaturation of TcTIM at three different temperatures followed by CD spectroscopy at 220 nm. Smooth lines are double exponential decay curves fitted to experimental data. Protein concentration was 0.010 mg mL^{-1} disolved in phosphate buffer at pH 7.4

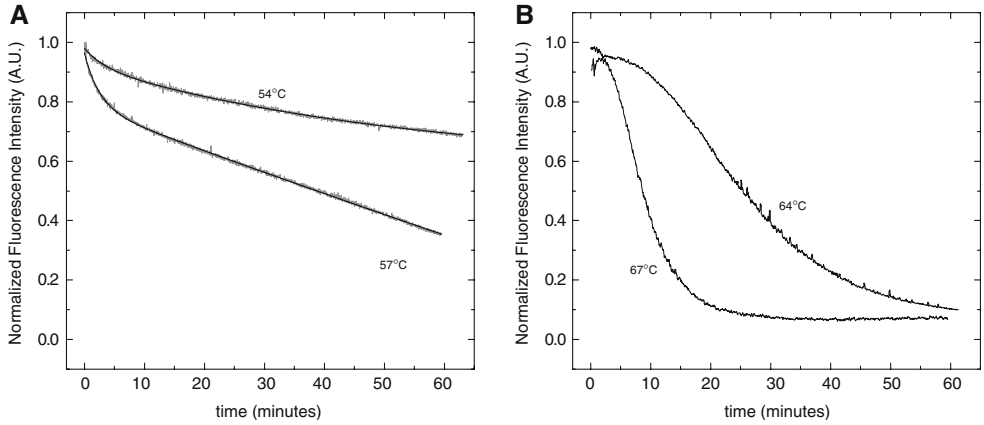

Fig. 3 Kinetics of thermal denaturation of TcTIM monitored by recording intrinsic fluorescence emission at 320 nm (excitation wavelength was 280 nm), at different temperatures. Panel (**A**) shows experiments recorded at 54 °C and 57 °C. Panel (**B**) shows experiments registered at 64 and 67 °C. Smooth lines in panel A are fittings of the data points to biphasic exponential decay equations. Protein concentration was 0.010 mg mL^{-1}

two different behaviours. Plots obtained at the lowest temperatures (51 (data not shown), 54 and 57 °C, Fig. 3 A) show a monotonic decrease of the emission intensity. These curves were fitted to biphasic exponential decay equations. The fittings allowed us to estimate values of the rate constants at different temperatures. In contrast, curves obtained at higher temperatures (above 60 °C, Fig. 3B) showed an initial kinetic phase which implies a small increment of the fluorescence-emission signal, followed by at least two phases that reduce the emission intensity at 320 nm. Fittings of these curves to double or triple decay equations were intended; nevertheless, the kinetic curves obtained at the highest temperatures showed very large fitting-errors. Therefore, the rate constants are not considered accurate for the discussion.

To further explore the changes in fluorescence signal, during thermal unfolding of TcTIM, emission spectra were obtained. The procedure for starting the series of spectra was the same as described for the kinetic curves, but instead of continuously monitoring a single emission wavelength, spectra were recorded at constant temperature every minute immediately after the temperature-jump. Figure 4 shows the very first spectrum for each kinetic experiment recorded in this way. It can be seen that those emission spectra recorded at the lower temperatures (51, 54 and 57 °C) do not show appreciable changes on the position of SCM (around 333 nm). On the contrary, the first spectrum registered at 61 °C clearly shows red-shifting of the SCM to 342 nm, and the spectra obtained at the higher temperatures (64 and 67 °C) show further red-shifting to larger wavelengths (349 nm). This indicates that there is an increment of the accessibility of tryptophanyl fluorophores to the solvent in the dead time of experiments [31–34].

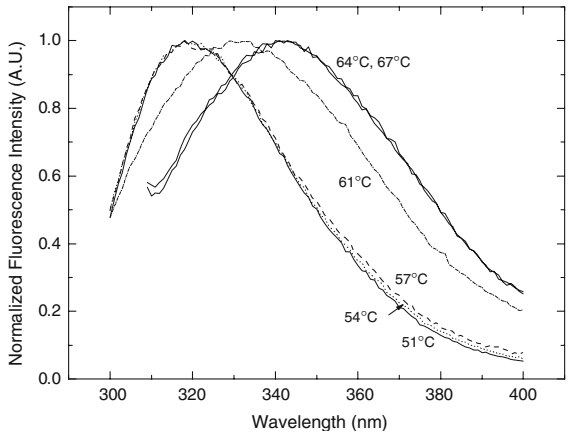

Fig. 4 Intrinsic fluorescence emission-spectra recorded immediately after temperature jump, at different temperatures. Protein concentration was 0.010 mg mL^{-1}. The excitation wavelength was 280 nm

3.4 Binding of a Hydrophobic Dye

The time course denaturation of TcTIM was also explored in the presence of ANS. The kinetic curves obtained at some of the temperatures studied (from 51 to 67 °C), of TcTIM solutions of 0.010 mg mL^{-1} in phosphate buffer, pH 7.4 and 40 μM concentration of ANS are shown in Fig. 5. It can be seen that again there are two different tendencies observed depending on the temperature studied. On one hand, the kinetic curves obtained at the lower temperatures (54 and 57 °C) showed an increment of ANS fluorescence, indicating the binding of ANS. These plots were fitted to single exponential decay equations, $\theta_t = \theta_f + A_1 \exp(-k_{u1}t)$ where θ_t is the ANS-fluorescence intensity measured at time t, θ_f is the final ANS-fluorescence value, A_1 represents the amplitude of the curve, and

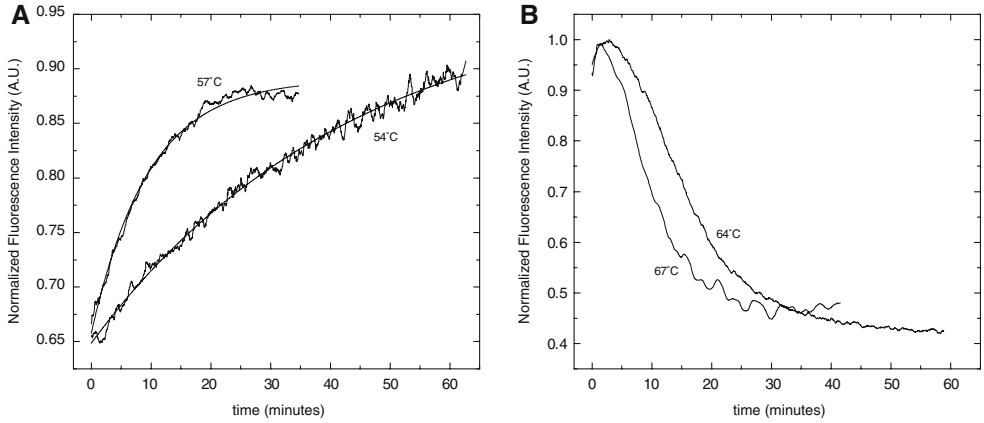

Fig. 5 ANS-Fluorescence emission kinetics at different temperatures. Panel (**A**) shows experiments recorded at 54 and 57 °C. Panel (**B**) shows experiments registered at 64 and 67 °C. Data points of panel A were fitted to monophasic exponential decay equations (smooth lines). TcTIM solutions were at a concentration of 0.010 mg mL^{-1} in phosphate buffer, pH 7.4. The concentration of ANS was 40 μM

k_{u1} is the rate constant associated to the binding of ANS. On the other hand, those curves registered at the higher temperatures (61, 64 and 67 °C) show a more complex mechanism. Firstly, an increment on the ANS-fluorescence emission is observed, followed by an important decrease of the signal. This result indicates that at high temperatures, the conformation that appears at the earliest stages of the TcTIM thermal-unfolding reaction binds ANS, followed by a step with species that looses the dye. Fittings of the curves obtained at the higher temperatures to exponential decay equations showed very large fitting errors; hence, kinetic constants are not discussed. Nevertheless, when comparing changes of intrinsic fluorescence and ANS-binding, qualitatively, it can be seen that the highest ANS fluorescence is observed when the intrinsic fluorescence intensity is already decreasing. This might be interpreted in terms of a loss of compactness in the molten globule state, or to aggregation of the sample. This type of molten globule-like intermediate has been observed before, in the unfolding of TcTIM caused by Gdn-HCl [6].

3.5 Temperature Dependence of the Unfolding Rate Constants

The effect of temperature on the rate constants of the reaction observed by changes in the secondary and tertiary structure for the denaturation of TcTIM (k_{u1}), as well as binding of ANS is illustrated in Fig. 6. The plotting of $\ln(k_u/T)$ vs. 1/T represents the Eyring's equation:

$$\ln(k_u/T) = \ln\ K_B/h + \Delta S^{\#}/R - (\Delta H^{\#}/R)(1/T) \qquad (1)$$

where, k_u is the rate constant of an elementary reaction; K_B and h are the Boltzman's and Planck's constants,

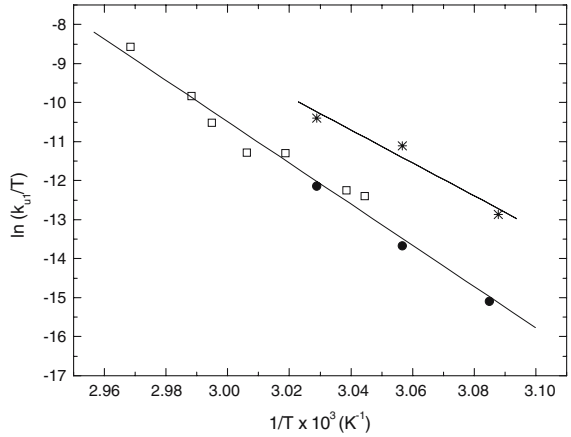

Fig. 6 Eyring's plots for the rate constants of unfolding (k_{u1}) of TcTIM. Denaturation data were obtained by means of far-UV CD (open squares), intrinsic fluorescence (stars) and ANS fluorescence (closed circles). Lines shown are least-squares regressions according to Eq. 1

respectively; $\Delta H^{\neq}$ and $\Delta S^{\neq}$ are the activation enthalpy and entropy, correspondingly. From Fig. 6 it is clear that the kinetic constants describe two linear or nearly linear plots of $\ln(k_u/T)$ vs. 1/T. The largest rate constants presented correspond to the fastest reaction detected by intrinsic fluorescence, whereas the reaction associated with changes on secondary structure and binding of ANS show smaller constants. The data obtained by means of far UV-CD and ANS fluorescence lay over the same linear trend, implying that these events could occur simultaneously. Linear or nearly linear plots of $\ln(k_u/T)$ vs. 1/T have been reported before for the unfolding reaction of monomeric proteins in aqueous solution, as well as previous studies on other TIMs, such as yTIM [22]. That is the case when the variation of $\Delta H^{\neq}$ with temperature ($\Delta C_p^{\neq}$) is practically negligible, indicating small changes in solvent accessibility

to reach the transition state. Fitting of unfolding data obtained by means of intrinsic fluorescence to Eq. 1 gave a $\Delta H^{\neq}$ value of 350 ± 74 kJ mol^{-1}, while fitting of far-UV CD and ANS binding data resulted in $\Delta H^{\neq}$ value of 430 ± 25 kJ mol^{-1}. In congruence, it has been reported that for yTIM, there is an enthalpic barrier of 480 kJ mol^{-1} [22]. Values of $\Delta H^{\neq}$ for monomeric proteins are comprised in the interval from 100 to 350 kJ mol^{-1} [35]. It could be proposed that one of the reasons that explain dimerization of enzymes might be the kinetic stability gained. Nevertheless, further cases are necessary for the generalization of this idea.

3.6 Description of the Mechanism and Comparison of the Unfolding Mechanism of TIM Barrels

According to the results showed above, the thermal denaturation of TcTIM is a complex-irreversible mechanism. The kinetics of the unfolding reaction might follow a sequential pathway.

The sequence of events observed at lower temperatures (below 60 °C), showed that TcTIM goes through changes in the environment of tryptophan residues (different from increment of exposure to the solvent) observed by decrease in the intensity of the fluorescence signal. Changes in the secondary structure observed by far-UV CD seem to come as a second step in the sequence of events. These changes are concomitant with ANS binding indicating the formation of a molten-globule like intermediate, accompanied by more changes on the environment of aromatic residues leading to the formation of the unfolded state. The changes of the secondary structure are followed by further changes in the fluorescence and CD signals, probably associated to aggregation of the sample. At higher temperatures (above 60 °C), the first change observed is the red-shift on the spectral centre of mass indicating the exposure of the tryptophanyl fluorophores to the solvent. These changes are accompanied by a slight increment of intrinsic fluorescence. The enhanced fluorescence might be due to alterations of the environment of aromatic fluorophores that decrease quenching. Subsequent reactions lead to the decrease in fluorescence intensity, binding and subsequent release of the hydrophobic dye and the loss of considerable part of the secondary structure of the molecule. It is important to point out that our results do not necessarily mean that pathways of TcTIM at different temperature ranges are dissimilar, but at higher temperatures the unfolding reaction occurs very rapidly and only the latest stages of the reaction could be observed. Although it was not possible to determine if the unfolding reaction is accompanied by dissociation of the dimer into monomers, it is very likely that dissociation is going on, based on previous reports on the thermal denaturation of yTIM and the Gdn-HCl induced unfolding of TcTIM [6, 22].

The structures of functional homologs are better conserved than their sequences. For this reason, in recent years there has been significant interest in investigating whether the protein folding mechanisms are conserved [5]. There are some authors that claim that topology is the main contributing factor in how a protein folds [36, 37]. If folding mechanisms were conserved, it would significantly simplify our view of folding and reduce the need to experimentally or computationally determine a pathway for every single protein of interest [38]. As it has been mentioned before, it has been found that yTIM showed a reversible thermal transition carried out at the same protein concentration as TcTIM. It was found that the unfolded state returns into native like TIM through a second-order reaction in which the association of the subunits is coupled to the recover of secondary structure. On the other hand, studies on Gdn-HCl induced unfolding of TcTIM, was found to be fully reversible showing the existence of two stable intermediates in the transition from the homodimeric native enzyme to the unfolded monomers: one is a slightly more expanded, non-native dimer, and the other is a partially expanded monomer that binds ANS [6]. On the opposite, in this work we have encountered that TcTIM exhibits a highly irreversible thermal-denaturation transition. The mechanism seems to be composed of consecutive reactions. Two kinetic (non-stable) intermediates were identified; nevertheless these intermediates are not structurally similar to those reported previously in the folding/unfolding reaction induced by Gdn-HCl. One of the kinetic intermediates shows altered environment of tryptophan residues, but maintains its secondary structure mostly intact, and the other with large changes on the secondary structure that binds ANS. Further conformational changes lead the loss of secondary structure and probably the aggregation of the unfolded conformation. At the highest temperatures studied, the unfolding reaction is so fast that the first steps might be lost during the dead time of experiments.

Acknowledgements We are very grateful to Dr. Armando Gomez Puyou and Beatriz Aguirre for the facilities and help given throughout the purification of TcTIM. EMH received financial support from Instituto Politécnico Nacional and PIFI-IPN (20050356 and 20060916), LMMV thanks economic sustain from CONACyT (175886). This work was supported by grants from TWAS (04–352 RG/BIO/LA), CONACyT (45990 and 46168-M), ECOS m05–501 and SIP-IPN 20070141.

References

1. Branden CI (1991) Curr Opin Struct Biol 1:978–983
2. Gromiha MM, Pujadas G, Magyar C, Selvaraj S, Simon I (2004) Proteins Struct Funct Bioinf 55:316–329

3. Orengo CA, Jones DT, Thornton JM (1994) Nature 372:631–634
4. Gualfetti JP, Masahiro I, Lee C, Kihara H, Bilsel O, Zitzewitz JA, Matthews CR (1999) Biochemistry 38:13367–13378
5. Forsyth WR, Matthews CR (2002) J Mol Biol 320:1119–1133
6. Chánez-Cárdenas ME, Pérez-Hernández G, Sánchez-Rebollar BG, Costas M, Vázquez-Contreras E (2005) Biochemistry 44:10883–10892
7. Bilsel O, Zitzewitz JA, Bowers KE, Matthews CR (1999) Biochemistry 38:1018–1029
8. Rojsajjakul T, Wintrode P, Vadrevu R, Matthews CR, Smith DL (2004) J Mol Biol 341: 241–253
9. Hocker B, Beismann-Driemeyer S, Hettwer S, Lustig A, Sterner R (2001) Nat Struct Biol 8:32–36
10. Mainfroid V, Mande SC, Hol WGJ, Martial JA, Goraj K (1996) Biochemistry 35:4110–4117
11. Beaucamp N, Hofmann A, Kellerer B, Jaenicke R (1997) Protein Sci 6:2159–2165
12. Rietveld AW, Ferreira ST (1996) Biochemistry 35:7743–7751
13. Moreau VH, Rietveld AWM, Ferreira ST (2003) Biochemistry 42:14831–14837
14. Pan H, Raza AS, Smith DL (2004) J Mol Biol 336:1251–1263
15. Gokhale RS, Ray SS, Balaram H, Balaram P (1999) Biochemistry 38:423–431
16. Vázquez-Contreras E, Zubillaga-Luna RA, Mendoza-Hernández G, Costas M, Fernández-Velasco DA (2000) Protein Pept Lett 7:57–64
17. Morgan CJ, Wilkins DK, Smith LJ, Kawata Y, Dobson CM (2000) Biochim Biophys Acta 1163:89–96
18. Nájera H, Costas M, Fernández-Velasco DA (2003) Biochem J 370:785–792
19. Lambeir AM, Backmann J, Ruiz-Sanz J, Filimonov V, Nielsen JE, Kursula I, Norledge BV, Wierenga RK (2000) Eur J Biochem 267:2516–2524
20. Chánez-Cárdenas ME, Fernandez-Velasco DA, Vázquez-Contreras E, Coria R, Saavedra-Rincón G, Pérez-Montfort R (2002) Arch Biochem Biophys 399:117–129
21. Téllez-Valencia A, Avila-Rios S, Pérez-Montfort R, Rodríguez-Romero A, Tuena de Gómez M, López-Calahorra F, Gómez-Puyou A (2002) Biochem Biophys Res Commun 295:958–963
22. Benítez-Cardoza CG, Rojo-Domínguez A, Hernández-Arana A (2001) Biochemistry 40:9049–9058
23. González-Mondragón E, Zubillaga-Luna RA, Saavedra-Lira E, Chánez-Cárdenas ME, Pérez-Montfort R, Hernández-Arana A (2004) Biochemistry 43:3255–3263
24. Ostoa-Saloma P, Garza-Ramos G, Ramírez J, Becker I, Berzunza I, Landa A, Gómez-Puyou A, Tuena de Gómez-Puyou M, Pérez-Montfort R (1997) Eur J Biochem 244:700–705
25. Pace CN, Vajdos F, Fee L, Grimsley G, Gray T (1995) Protein Sci 4:2411–2423
26. Freire E, van Osdol WW, Mayorga OL, Sanchez-Ruiz JM (1990) Annu Rev Biophys Biophys Chem 19:159–188
27. Sánchez-Ruiz JM (1992) Biophys J 61:921–935
28. Tello-Solís SR, Hernández-Arana A (1995) Biochem J 311: 969–974
29. Milardi D, La-Rosa C, Grasso D (1994) Biophys Chem 52: 183–189
30. Goins B, Freire E (1988) Biochemistry 27:2046–2052
31. Demchenko AP (1988) Eur Biophys J 16:121–129
32. Demchenko AP, Ladokhin AS (1988) Eur Biophys J 15:369–379
33. Chen Y, Barkley MD (1998) Biochemistry 37:9976–9982
34. Pattanaik P, Ravindra G, Sengupta C, Maithal K, Balaram P, Balaram H (2003) Eur J Biochem 270:745–756
35. Solís-Mendiola S, Gutiérrez-González LH, Arroyo-Reyna A, Padilla-Zuñiga J, Rojo-Domínguez A, Hernández-Arana A (1998) Biochim Biophys Acta 1388:363–372
36. Plaxco KW, Simons KT, Baker D (1998) J Mol Biol 277: 985–994
37. Plaxco KW, Larson S, Ruczinski I, Riddle DS, Thayer EC, Buchwitz B, Davidson AR, Baker D (2000) J Mol Biol 298: 303–312
38. Baker D (2000) Nature 405:39–42